Life Sciences 239 (2019) 117034

Contents lists available at ScienceDirect

Life Sciences

journal homepage: www.elsevier.com/locate/lifescie

METTL14-dependent m6A regulates vascular calcification induced by indoxyl sulfate

Jing Chen[a,b,c,d,e], Yichun Ning[a,b,c,d,e], Han Zhang[a,b,c,d,e], Nana Song[a,b,c,d,e], Yulu Gu[c,d,e], Yiqin Shi[a,b,c,d,e], Jieru Cai[a,b,c,d,e], Xiaoqiang Ding[a,b,c,d,e,**], Xiaoyan Zhang[a,b,c,d,e,*]

[a] Department of Nephrology, Zhongshan Hospital, Fudan University, China
[b] Shanghai Medical Center of Kidney, China
[c] Shanghai Institute of Kidney and Dialysis, Shanghai, China
[d] Shanghai Key Laboratory of Kidney and Blood Purification, Shanghai, China
[e] Hemodialysis quality control center of Shanghai, China

ARTICLE INFO

Keywords:
CKD
Vascular calcification
Indoxyl sulfate
Klotho
RNA methylation

ABSTRACT

Aims: Although the functional importance of N6-methyladenosine (m6A) in various fundamental bioprocesses are well known, its effect on vascular calcification is not well studied. We investigated the role of methyltransferase-like 14 (METTL14), an m6A methylase, in vascular calcification.

Main methods: We used clinical human samples as well as rat models and primary human artery smooth muscle cell (HASMC) cultures to study the functional role of m6A and METTL14 in vascular calcification and in HASMCs. We modulated the expression of METTL14 using siRNAs (*in vitro*) to study its function in regulating HASMCs m6A, osteoblasts induced by indoxyl sulfate. We performed the MeRIP-qPCR assays to map and validate m6A in individual transcripts, controls, and calcific HASMCs.

Key findings: We discovered that the METTL14 expression increases in calcific arteries and in HASMCs induced by indoxyl sulfate, thereby increasing the m6A level in RNA and decreasing the vascular repair function. Decreasing the expression of METTL14 in calcified arteries attenuated the indoxyl sulfate-induced increase in m6A and decrease in HASMCs calcification. We performed the methylation activity of METTL14, which selectively methylates vascular osteogenic transcripts, thereby promoting their degradation and improving their protein expression induced by indoxyl sulfate. Moreover, we demonstrated that the METTL14 de-expression in HASMCs models of calcification decreased the calcification and enhanced the vascular repair function.

Significance: Collectively, our results demonstrated the functional importance of METTL14-dependent vascular m6A methylome in vascular functions during calcification and provided a novel mechanistic insight to the therapeutic mechanisms of METTL14.

1. Introduction

Chronic kidney disease (CKD) is usually regarded as a permanent loss of kidney functions. The mortality rate of cardiovascular disease is significantly higher in patients with CKD than in the general population [1,2]. Accelerated vascular calcification is considered as one of the major causes of this elevated mortality rate [3,4]. Protein-bound uremic toxins indoxyl sulfate (IS) has been associated with cardiovascular morbidity and mortality in patients with CKD.

Although the available therapy has been proved to slow down the progress of arterial calcification, the pathophysiological mechanism of treating vascular calcification remains unknown. The current therapeutic approaches have demonstrated limited success in treating vascular calcification in CKD patients. Therefore, newer concepts for vascular calcification that improves the vascular function need to be developed.

Recent findings in this field suggest that the most abundant internal chemical modification in RNA N6-methyladenosine (m6A) is a critical regulator of mRNA stability, protein expression, and several other cellular processes [5–8]. Although dysregulated m6A has been associated

* Corresponding author. Kidney and Dialysis Institute of Shanghai, No 136 Medical College Road, Shanghai 200032, China.
** Corresponding author. Shanghai Key Laboratory of Kidney and Blood Purification, Shanghai, China.
E-mail addresses: ding.xiaoqiang@zs-hospital.sh.cn (X. Ding), zhang.xiaoyan@zs-hospital.sh.cn (X. Zhang).

https://doi.org/10.1016/j.lfs.2019.117034
Received 12 August 2019; Received in revised form 24 October 2019; Accepted 30 October 2019
Available online 04 November 2019
0024-3205/

with various cancer types [9,10] and brain diseases [10,11], its role in vascular homeostasis and calcification induced via uremic toxins such as indoxyl sulfate remains to be studied. Therefore, we investigated the epitranscriptomic regulations underlying vascular calcification induced by indoxyl sulfate and found a predominant but previously unidentified mechanism, which contributes to vascular calcification via dysregulated RNA modifications.

Several recent reports suggest that epitranscriptomic mRNA modifications are reversible and can be dynamically regulated with dedicated writers (i.e., methyltransferases) that catalyze the addition of m6A (i.e., methyltransferase-like 3 [METTL3], METTL4, METTL14, and WTAP) and dedicated erasers (i.e., demethylases), which catalyze the removal of m6A (i.e., FTO and ALKBH5) from mRNA [12,13]. METTL14 protein has been reported to play the key role in regulating transcriptome-wide m6A modification in mRNAs [5,13]and also as one of the m6A regulators associated with cancers.

Until date, although the function of m6A in the physiological and biological processes has been investigated, studies on the m6A level under pathological conditions, especially in tissues and organs, remain limited. Moreover, METTL14-dependent m6A methylation and its role in vascular protein expression and function in healthy and calcified arteries remain to be addressed. We used clinical human samples, preclinical rat models of uremic calcification, and primary human artery smooth muscle cells (HASMCs) culture to investigate the physiological and pathological roles of METTL14-dependent m6A epitranscriptome in vascular homeostasis, remodeling, and repair. We have presented evidence that m6A in RNA is dysregulated in vascular calcification and that METTL14-dependent m6A plays a significant role in the pathomechanisms of vascular calcification at the molecular (i.e., in mRNA degradation and protein expression), cellular, and organ levels. Moreover, we demonstrated that *METTL14* delivery attenuates the indoxyl sulfate-induced vascular calcification, thereby demonstrating the therapeutic potential of METTL14 in the treatment of uremic calcification. Mechanistically, METTL14 selectively methylates vascular-protecting transcripts, promoting their degradation and regulating their protein expression in vascular calcification. Our study helped uncover the novel function of METTL14-regulated m6A mechanisms in uremic vascular remodeling and repair. Through our study, we could also establish that targeting vascular epitranscriptome via METTL14 can be an effective therapeutic strategy for uremic calcification.

2. Methods

The data, analytic methods, and study materials will be made available to other researchers for the purposes of reproducing the results or for replicating the procedure.

2.1. Study design

The human radial arteries were collected from the patients with end-stage renal disease (ESRD) undergoing arteriovenostomy for hemodialysis. The radial arteries harvested as grafts from age- and sex-matched patients with coronary heart diseases undergoing coronary artery bypass graft served as control. Human artery collection was conducted at the Zhongshan Hospital, Fudan University, Shanghai, China. Ethical approval was obtained from the Clinical Research Ethical Committee of the hospital, and the procedures were conducted in accordance with the approved guidelines. The patients provided their written informed consent for the use of their tissues for research purposes. All subjects provided written informed consent in accordance with the Declaration of Helsinki.

Eight-week-old SD rats with 5/6-nephrectomy were used in this study [14]. The experimental rats received intraperitoneal injection with IS (Alfa Aesar, Lancashire, England; n = 5) at a dosage of 100 mg/kg/48 h [15,16] for 8,16,24 weeks. The control rats (n = 5) received same volume of phosphate-buffered saline injection every 48 h for 8,16,24 weeks. At the end of study, the body weight of study animal was recorded and the serum levels of blood urea nitrogen (BUN) and creatinine (Cr) were analyzed. The aortic tissue was micro dissected for further analysis. This study was approved by the Institutional Animal Care and Use Committee and performed in accordance with the NIH Guide for the Care and Use of Laboratory Animals. Surgery was performed under sodium pentobarbital anesthesia to minimize the pain incurred to animals. The flow diagram for animal study is summarized in Figure S1 in the online-only Data Supplement.

HASMCs were obtained from the ScienCell Research Laboratory (CA, USA). The rats were cultured in an incubator at 37 °C under 5% CO_2 atmosphere using a smooth muscle cell medium supplemented with 5% fetal bovine serum. HASMCs cultured at approximately 70% confluence were synchronized under serum-free conditions for 48 h and then treated with IS at the concentrations of 0, 200, 500, and 1000 μmol/L for 72 days. Knockdown of METTL14 was achieved by transfection of siRNA targeting METTL14 (TriFECTa Mettl14 RNAi by IDT) or negative siRNA control (TriFECTa negative control DS NC1 RNAi by IDT), and the cells were analyzed 48 h after the transfection. The overexpression of METTL14 or β-galactosidase (control) was achieved via adenoviral infection, and the cells were analyzed 48 h after the infection.

2.2. RNA isolation

Total RNA isolation for UPLC-MS/MS analysis: total RNA was isolated with Trizol reagent (Invitrogen). mRNA was extracted using the GenElute mRNA Miniprep (Sigma-Aldrich), followed by further removal of the contaminated rRNAs using the RiboMinus Transcriptome Isolation Kit (Invitrogen) according to the manufacturer's instructions. The mRNA concentration was measured by Qubit.

2.3. UPLC-MS/MS analysis of m6A

About 50–100 ng of purified mRNA was digested with nuclease P1 (1 U; Sigma) in 20 μL of buffer containing 10 mM of NH4Ac (pH 5.3) at 42 °C for 4 h. About 100 mM NH_4HCO_3 and alkaline phosphatase (0.5 U) were then added to the reaction mixture and incubated for another 4 h at 37 °C. The digested sample was centrifuged at 4 °C, 13,000 rpm for 20 min, and the resultant supernatant was injected into UPLC-MS/MS. The nucleosides were separated by UPLC (SHIMADZU) equipped with the ZORBAX SB-Aq column (Agilent) and detected with the Triple Quad 5500 (AB SCIEX) in the positive ion multiple reaction-monitoring mode. The quantitation of modifications was based on nucleoside-to-base ion mass transitions: *m/z* 268.0–136.0 for A and *m/z* 282.0–150.1 for m6A. Pure nucleosides were used to generate the standard curves, from which the concentrations of A and m6A in the sample were calculated. The level of m6A was then calculated as a percent of total unmodified A.

2.4. Western blot analyses

Total protein was extracted using a commercial kit (Protein Extraction Kit, Millipore) and 30 μg total protein from each sample was loaded onto separate lanes of 10% sodium dodecylsulfate-poly-acrylamide gel. Proteins were electrotransferred onto polyvinylidene fluoride membranes (0.2 mm: Immun-Blot, Bio-Rad) and immunoblotted with specific antibodies listed in Table S2 on Supplementary material. The intensity of each band was quantified using NIH Image J software (Bethesda, MD) and then normalized against GAPDH expression.

2.5. Immunohistochemistry staining

Immunohistochemistry staining was performed using a biotin-streptavidin-peroxidase method. Rabbit anti-METTL14 (1:200; Abcam) was used as primary antibodies. Biotinylated goat anti-rabbit

immunoglobulin G was used as the secondary antibody. The sections incubated with non-immune rabbit or mouse serum instead of the primary antibodies served as negative controls. All sections were stained under identical conditions together with the controls. Nuclei were lightly counterstained with hematoxylin.

2.6. Alizarin Red S staining

Alizarin Red S staining was used for calcium deposition evaluation. Paraffin-embedded artery rings were sectioned into 4-μm-thick sections, deparaffinized and then stained in 1 mg/ml Alizarin Red S solution (Sigma, St. Louis, MO, USA) (pH 4.0–4.2). For HASMCs, cells were washed with 0.9% NaCl isotonic solution, fixed with 4% paraformaldehyde for 15 min, rinsed, and stained with Alizarin Red S solution for 30 min. The results were observed under light-microscopy and photographed by digital camera. Positive results were shown in an orange-red color in light microscope. Calculation of relative calcification area based on positive staining area.

2.7. Methylated RNA immunoprecipitation and MeRIP-qPCR

Briefly, 200 μg of human total RNA was used. Total RNA were isolated for polyA$^+$RNA (Promega) and then RNA-quantified. PolyA$^+$ RNA was fragmented to approximately 100 nt long fragments in RNA fragmentation buffer (Millipore Sigma). RNA fragmentation was ensured by using a bioanalyzer before proceeding to m6A-IP. Non-IP RNA was stored from fragmented RNA for bioinformatics analysis. For MeRIP-qPCR, immunopurified RNA was purified and first-strand cDNA synthesis was performed as described earlier. The enrichment of mRNA in m6A-immunopurified samples was expressed relative to the 18s rRNA in the bound samples and expressed as a fold change between the groups.

2.8. Statistical methods

Data are shown as mean ± SEM, unless otherwise stated. One-way analysis of variance (ANOVA) was used to determine the statistical significance for experiments with more than two groups, followed by Bonferroni's post-hoc tests. Figures with ANOVA analysis where applicable are indicated in the corresponding figure legends. Comparison between the two groups was performed using the GraphPad software with an unpaired Student's t-test. $P < 0.05$ was considered statistically significant and assigned in individual figures.

3. Results

3.1. Increased m6A RNA in human and rat vascular calcification

We quantified the m6A levels in RNA extracted from ESRD human and rat arteries and then compared them with the m6A levels in control human and sham surgical controls, respectively. We detected significantly elevated levels of m6A in total RNA extracted from humans, and the levels were compared between that in rat calcified arteries and non-calcific or sham controls (Fig. 1A–B). We observed a sustained increase in the m6A level in total RNA in the chronic phases of ESRD-related vascular calcification in rat calcific vascular measured at 8 and 24 weeks, respectively (Fig. 1B). These results provide strong evidence of increases in the m6A level in RNA in ESRD conditions in humans, which were conserved across the species in rats.

3.2. Increased Mettl14 expression in human and rat vascular calcification

To identify the regulators of elevated m6A in vascular calcification, we measured the expression levels of several known RNAs and proteins associated with m6A methylation (writers such as METTL3, METTL4, and METTL14 and their regulatory subunit, WTAP) and demethylation (erasers such as FTO and ALKBH5) in human and rat aortic artery. Western blotting and qRT-PCR data revealed that the expression of METTL14 (for human; for rat: METTL14) was significantly increased in calcified arteries from human and rat samples, both at the RNA and the protein levels as compared with their respective control values (Fig. 2A–F). The increase of METTL14 was detected in uremic rat calcific aortic artery, and the increase in METTL14 mRNA and protein levels consistently correlated with the increased m6A level (Fig. 2D–E). Moreover, the transient and inconsistent increase or decrease of other m6A writers and erasers (Fig. 2F) could not fully explain the aberrant and sustained increase in the m6A level in the calcified arteries. Interestingly, among all the m6A writers and erasers studied, METTL14 showed the highest baseline expression both at the RNA and protein levels in healthy human (Fig. 2A) and no-surgery rat (Fig. 2B) vascular tissues. Collectively, these data established that indoxyl sulfate-induced increase of METTL14 could be an important molecular hallmark that may explain the increase in the m6A levels in human and rat calcified arteries.

3.3. Mettl14-dependent m6A methylation regulates osteoblasts in HASMCs

To investigate the role of METTL14 in vascular smooth muscle cells and to determine whether METTL14 is a direct regulator of m6A, we established cell culture models with the loss of METTL14 using siRNA to METTL14 (siMETTL14) and the gain of METTL14 using adenovirus carrying METTL14 (adMETTL14) in the HASMCs and in comparison with those in si-Ctrl and adnull controls, respectively (Fig. 3A). Interestingly, the expression of METTL14 correlated with the m6A level in total RNA in primary HASMCs (Fig. 3A and B). Similar to that in calcified rats and human arteries, primary HASMCs subjected to indoxyl sulfate increased the m6A level in RNAs (Figs. 3B and 4B). De-expressing Mettl14 in HASMCs cultured under indoxyl sulfate reversed the induced aberrant increase in the m6A level in RNA (Fig. 3B), suggesting that Mettl14 is the key regulator of m6A levels in HASMCs.

3.4. Klotho transcripts hypermethylated in calcified arteries are methylated by Mettl14 overexpression

PCR analyses of MeRIP-enriched RNA from human calcific arteries confirmed that the arteries preventing transcripts Klotho was hypermethylated (Fig. 5A). Consistent with this, Klotho mRNA was demethylated when Mettl14 was de-expressed in HASMCs (Fig. 5B), resulting in increased Klotho mRNA expression (Fig. 5B). The hypermethylation of Klotho mRNA and its association with decreased mRNA levels could be a result of METTL14 increasing the degradation of Klotho mRNA and possibly of other vascular-protecting mRNAs.

The quantification of m6A level in total RNA in the arteries of A, human, n = 6–11; from 5/6 Ne rat calcific area in B, rat, n = 3–6. Error bars represent SEM. *P < 0.05, compared with control or sham. C and D, Alizarin red calcium staining of arteries from ESRD patients and 5/6Ne rats. Reddish/purple staining indicated mineral deposition.

A, quantification of mRNA, n = 3–6; B, representative immunohistochemistry; C, quantification of mRNA, n = 3–7; D, densitometry quantification of protein, n = 3–7 for m6A regulators at different time points in rat aortic artery; D, representative immunoblots; and E, densitometry quantification of Mettl14, n = 3–4. F, qRT-PCR quantification of selected mRNA expressions in rat aortic artery, n = 4–8. Error bars represent SEM. *P < 0.05, **P < 0.01, compared with non-failing or sham.

A, qPCR analysis for METTL14 expression in response to Ctrl or METTL14 siRNA mediated knockdown (n = 3 each). B, m6A in total RNA of smooth muscle cells treated with control siRNA (si-Ctrl) or siRNA targeting METTL14 (si-M14). C, Quantification of smooth muscle cells area (n ≥ 50 cells/well, n = 3 independent experiments/treatment). *P < 0.05 versus control; #P < 0.05 versus si-Ctrl.

Quantification of A, Mettl14 mRNA, n = 3–4; B, m6A in total RNA,

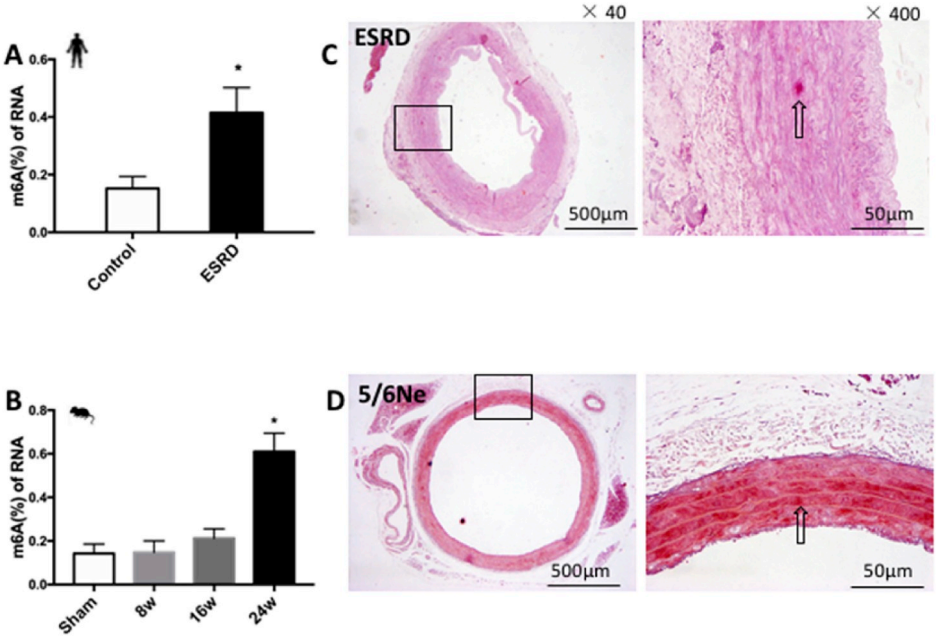

Fig. 1. Increased m6A level in RNA in ESRD patients and rat calcified vasculars.

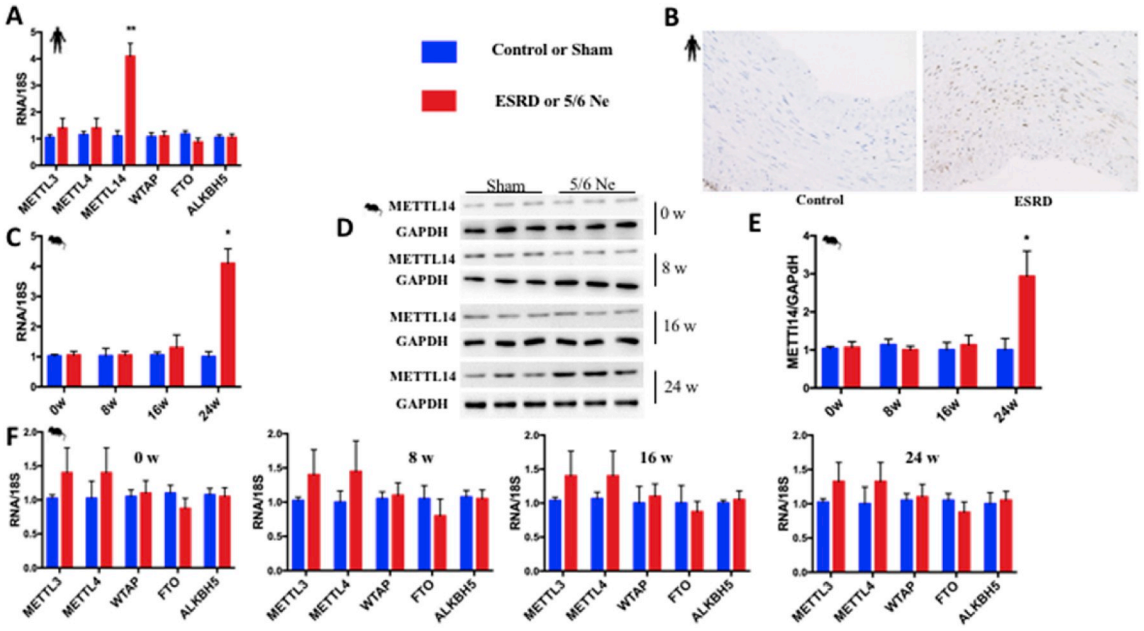

Fig. 2. Increased Mettl14 mRNA and protein expressions in human and rat calcified arteries.

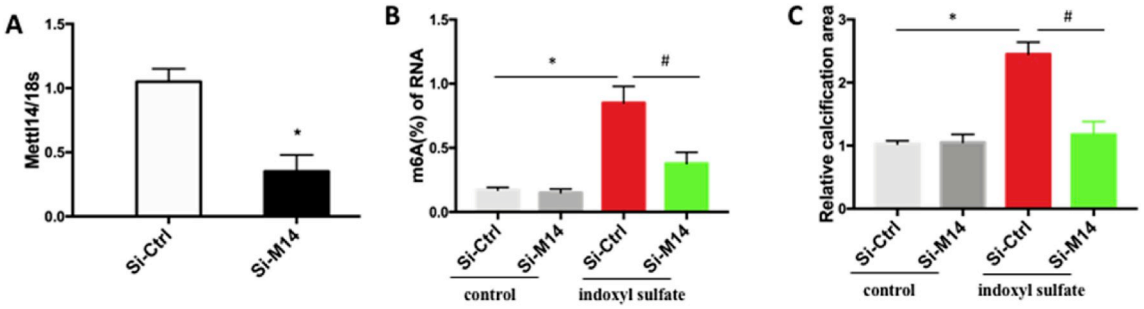

Fig. 3. METTL14 inhibition prevents the development of vascular calcification induced by indoxyl sulfate.

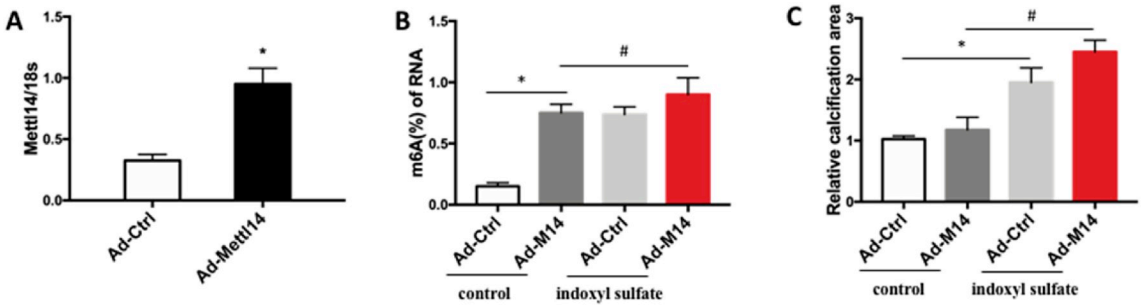

Fig. 4. Mettl14-mediated m6A methylation regulates the smooth muscle cells osteoblast conversion.

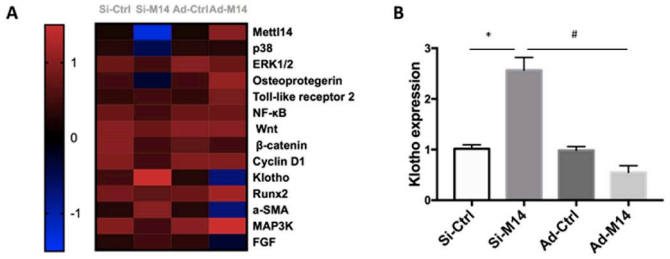

Fig. 5. Klotho mRNA is hypermethylated in human smooth muscle cells and methylation by Mettl14 overexpression induces the Klotho mRNA de-expression.

n = 3–5; C, representative calcification areas induced by indoxyl sulfate, n = 3.

A, human MeRIP-qPCR showing m6A enrichment in mRNA. B, Klotho mRNA, n = 3 expressions in human smooth muscle cells. *P < 0.05, ***P < 0.001.

4. Discussion

Chronic kidney disease (CKD) is now clearly recognized as a public health problem worldwide. Patients with CKD display a substantial increase in end-stage renal disease (ESRD) and cardiovascular disease (CVD) [17]. Moreover, the prognosis of CVD in CKD is extremely poor [18]. Understanding the pathophysiology of CVD in CKD might help to develop treatment strategies to reduce its morbidity and mortality [19]. Compelling evidence suggests that the uremic milieu itself plays a critical role in the development and progression of CVD [20]. Indoxyl sulfate, a uremic toxin, has been associated with CVD in patients with CKD [21–25]. Vascular calcification is one of important phenotypes of CVD in CKD. Investigation of the underlying mechanism of IS-induced vascular calcification will be essential for new treatment strategy.

Patients with CKD suffer from more extensive calcification than the general population [26–28]. IS is one of the most important protein-bound uremic toxins and is recognized as one of the major risk factors of vascular calcification in CKD. In the past, many studies have focused on the signaling pathways leading to activation of VSMCs proliferation, osteogenesis transformation, and senescence [29–32]. Although significant progress has been made in understanding the transcriptional control of gene expression during vascular calcification, it is now clear that post-transcriptional regulation of protein expression is a similarly critical mechanism for cardiovascular disease. For example, microRNA-mediated gene silencing are established mechanisms of gene expression that directly alter protein levels in vascular calcification. It is now clear that m6A methylation plays important and diverse biological functions in hypertrophic control [33]. The underlying mechanisms of how IS regulates RNA m6A are still unclear.

The control of protein synthesis can be achieved via complex and poorly defined mechanisms that regulate the vascular calcification processing of mRNAs. Understanding how the specific classes of functionally related mRNAs are co-regulated in the vascular system is crucial for the elucidation of the molecular mechanisms controlling the characteristic increase in CKD patients that defines the vascular calcification within smooth muscle cells. In this study, we noted compelling *in vitro*, *in vivo*, and translational evidence demonstrating the important role for Mettl14 in vascular calcification induced by indoxyl sulfate. We identified Mettl14 as the key vascular methylase that regulates vascular m6A and provided the novel characterization of Mettl14-dependent m6A in vascular calcification induced by indoxyl sulfate. The Mettl14 expression is upregulated in calcific arteries, leading to aberrant increase in the global vascular m6A level as well as the m6A level in selective osteoblast-related transcripts leading to their decreased protein expression. Increased Mettl14 expression resulted in the loss of repair functions in primary HASMCs. Interestingly, the forced expression of Mettl14 in stressed HASMCs attenuated indoxyl sulfate-induced calcification, loss of vascular-protecting protein expression, and the loss of vascular repair function. Our study demonstrated the functional importance of Mettl14-dependent vascular m6A methylome in vascular repair function and calcification during CKD as well as provided robust mechanistic insights to the therapeutic potential of Mettl14.

By modulating the Mettl14 expression through silencing or overexpression in isolated primary HASMCs, we demonstrated that Mettl14 is the key contributor of global m6A levels. Furthermore, the Mettl14 expression correlated with the m6A level, and Mettl14-dependent m6A level is a novel and negative regulator of smooth muscle cells and vascular repair function. A recent study investigated the Mettl14 expression in myoblast differentiation and revealed that Mettl14 depletion interfered with myogenic differentiation, which highlighted that Mettl14 is required for myogenesis [34]. These data implicate the important role of Mettl14 as a regulator of muscle physiology.

The m6A modification forms a part of the larger field of RNA epigenetics, which is a growing field that has only recently been explored in the heart. Similar to the deposition of epigenetic marks on DNA, the methylation of mRNAs can impact the gene expressivity and define the fate of mRNAs subgroups. Indeed, transcription is a time-consuming process, and the cells have devised methods to preserve pools of mRNAs that can be made readily and dynamically available for translation. As m6A demethylation in a single-stranded nuclear RNA is the only known primary function of Mettl14, we attribute the effects of Mettl14 alteration directly to the changes in the m6A levels in the target transcripts. Nevertheless, we did not eliminate Mettl14-dependent N6,2′-O-dimethyladenosine (m6Am) methylation, long noncoding RNA methylation, or other indirect effects resulting from Mettl14 (m6A)-regulated transcriptional co-regulatory networks or miRNA expression. Moreover, in addition to Mettl14 upregulation, we detected decreased levels of eraser proteins, such as FTO in human and ALKBH5 in mouse calcified arteries, which suggests that these erasers possibly also contribute to the increased m6A level in calcified arteries. However, whether these erasers compete with Mettl14 to target similar subsets and locations of transcripts or functions in a mutually exclusive manner remains to be investigated. The increase in transcriptome-wide m6A level was significant only at 24 weeks post-5/6Ne, and the Mettl14 expression was

upregulated as early as 24 weeks post-5/6Ne. As m6A is dynamically regulated, the interplay between writer, eraser, and reader proteins could be important in regulating the protein expression during vascular repair and regeneration and therefore needs to be determined.

Together, our data provides proof of principle that given the functional importance of Mettl14 in IS-induced vascular calcification, targeting Mettl14 signaling may represent a promising therapeutic strategy to treat IS-induced vascular calcification. The underlying mechanisms of how Mettl14 regulates Klotho in VSMCs still need investigation.

Funding sources

This study was supported by research grants 81600579, 81700646 from National Natural Science Foundation of China. 19YF1406700 from Shanghai Sailing Program. Shanghai Municipal Health Commission(2017ZZ01015). The Science and Technology Commission of Shanghai Municipality (14DZ2260200, the project of Shanghai Key Laboratory of Kidney and Blood Purification).

Declaration of competing interest

The authors have declared that no competing interest exists.

Appendix A. Supplementary data

Supplementary data to this article can be found online at https://doi.org/10.1016/j.lfs.2019.117034.

References

[1] B. Thomas, K. Matsushita, K.H. Abate, Z. Al-Aly, J. Ärnlöv, K. Asayama, Global cardiovascular and renal outcomes of reduced GFR, J. Am. Soc. Nephrol. 28 (2017) 2167–2179.
[2] C.M. Shanahan, M.H. Crouthamel, A. Kapustin, C.M. Giachelli, Arterial calcification in chronic kidney disease: key roles for calcium and phosphate, Circ. Res. 109 (2011) 697–711.
[3] G.M. London, A.P. Guérin, S.J. Marchais, F. Métivier, B. Pannier, H. Adda, Arterial media calcification in end-stage renal disease: impact on all- cause and cardiovascular mortality, Nephrol. Dial. Transplant. 18 (2003) 385–389.
[4] J. Blacher, A.P. Guerin, B. Pannier, S.J. Marchais, G.M. London, Arterial calcifications, arterial stiffness, and cardiovascular risk in end-stage renal disease, Hypertension 38 (2001) 938–942.
[5] K.D. Meyer, Y. Saletore, P. Zumbo, O. Elemento, C.E. Mason, S.R. Jaffrey, Comprehensive analysis of mRNA methylation reveals enrichment in 3' UTRs and near stop codons, Cell 149 (2012) 1635–1646.
[6] Y. Fu, D. Dominissini, G. Rechavi, C. He, Gene expression regulation mediated through reversible m(6)A RNA methylation, Nat. Rev. Genet. 15 (2014) 293–306.
[7] X. Wang, Z. Lu, A. Gomez, G.C. Hon, Y. Yue, D. Han, et al., N6-methyladenosine-dependent regulation of messenger RNA stability, Nature 505 (2014) 117–120.
[8] N. Liu, K.I. Zhou, M. Parisien, Q. Dai, L. Diatchenko, T. Pan, N6-methyladenosine alters RNA structure to regulate binding of a low-complexity protein, Nucleic Acids Res. 45 (2017) 6051–6063.
[9] S. Zhang, B.S. Zhao, A. Zhou, K. Lin, S. Zheng, Z. Lu, et al., m6A demethylase ALKBH5 maintains tumorigenicity of glioblastoma stem-like cells by sustaining FOXM1 expression and cell proliferation program, Cancer Cell 31 (2017) 591–606 e6.
[10] Z. Li, H. Weng, R. Su, X. Weng, Z. Zuo, C. Li, et al., FTO plays an oncogenic role in acute myeloid leukemia as a N(6)-methyladenosine RNA demethylase, Cancer Cell 31 (2017) 127–141.
[11] M.E. Hess, S. Hess, K.D. Meyer, L.A. Verhagen, L. Koch, H.S. Bronneke, et al., The fat mass and obesity associated gene (Fto) regulates activity of the dopaminergic midbrain circuitry, Nat. Neurosci. 16 (2013) 1042–1048.
[12] B.S. Zhao, I.A. Roundtree, C. He, Post-transcriptional gene regulation by mRNA modifications, Nat. Rev. Mol. Cell Biol. 18 (2017) 31–42.
[13] G. Jia, Y. Fu, X. Zhao, Q. Dai, G. Zheng, Y. Yang, et al., N6-methyladenosine in nuclear RNA is a major substrate of the obesity-associated FTO, Nat. Chem. Biol. 7 (2011) 885–887.
[14] C.Y. Sun, S.C. Chang, M.S. Wu, Suppression of Klotho expression by protein-bound uremic toxins is associated with increased DNA methyltransferase expression and DNA hypermethylation, Kidney Int. 81 (2012) 640–650.
[15] A. Adijiang, S. Goto, S. Uramoto, Indoxyl sulphate promotes aortic calcification with expression of osteoblast-specific proteins in hypertensive rats, Nephrol. Dial. Transplant. 23 (2008) 1892–1901.
[16] J. Chen, X.Y. Zhang, H. Zhang, T.Q. Liu, H. Zhang, J. Teng, et al., Indoxyl sulfate enhance the hypermethylation of Klotho and promote the process of vascular calcification in chronic kidney disease, Int. J. Biol. Sci. 12 (2016) 1236–1246.
[17] C.P. Wen, T.Y. Cheng, M.K. Tsai, Y.C. Chang, H.T. Chan, S.P. Tsai, et al., All cause mortality attributable to chronic kidney disease: a prospective cohort study based on 462293 adults in Taiwan, Lancet 371 (2008) 2173–2182.
[18] A. Levin, R.N. Foley, Cardiovascular disease in chronic renal insufficiency, Am. J. Kidney Dis. 36 (2000) S24–S30.
[19] Szu-Chun Hung, Ko-Lin Kuo, Chih-Cheng Wu, Der-Cherng Tarng, Indoxyl sulfate: a novel cardiovascular risk factor in chronic kidney disease, J Am Heart Assoc 6 (2017) e005022.
[20] R. Vanholder, E. Schepers, A. Pletinck, E.V. Nagler, G. Glorieux, The uremic toxicity of indoxyl sulfate and p-cresyl sulfate: a systematic review, J. Am. Soc. Nephrol. 25 (2014) 1897–1907.
[21] X.S. Cao, J. Chen, J.Z. Zou, Y.H. Zhong, J. Teng, J. Ji, et al., Association of indoxyl sulfate with heart failure among patients on hemodialysis, Clin. J. Am. Soc. Nephrol. 10 (2015) 111–119.
[22] B. Bammens, P. Evenepoel, H. Keuleers, K. Verbeke, Y. Vanrenterghem, Free serum concentrations of the protein-bound retention solute p-cresol predict mortality in hemodialysis patients, Kidney Int. 69 (2006) 1081–1087.
[23] B.K. Meijers, B. Bammens, B. De Moor, K. Verbeke, Y. Vanrenterghem, P. Evenepoel, Free p-cresol is associated with cardiovascular disease in hemodialysis patients, Kidney Int. 73 (2008) 1173–1180.
[24] B.K. Meijers, K. Claes, B. Bammens, H. de Loor, L. Viaene, K. Verbeke, et al., p-Cresol and cardiovascular risk in mild-to-moderate kidney disease, Clin. J. Am. Soc. Nephrol. 5 (2010) 1182–1189.
[25] J.R. Stubbs, J.A. House, A.J. Ocque, S. Zhang, C. Johnson, C. Kimber, et al., Serum trimethylamine-N-oxide is elevated in CKD and correlates with coronary atherosclerosis burden, J. Am. Soc. Nephrol. 27 (2016) 305–313.
[26] Y. Fang, C. Ginsberg, T. Sugatani, M.C. Monier-Faugere, H. Malluche, K.A. Hruska, Early chronic kidney disease-mineral bone disorder stimulates vascular calcification, Kidney Int. 85 (2014) 142–150.
[27] S.M. Moe, N.X. Chen, Pathophysiology of vascular calcification in chronic kidney disease, Circ. Res. 95 (2004) 560–567.
[28] E. Neven, P.C. D'Haese, Vascular calcification in chronic renal failure: what have we learned from animal studies? Circ. Res. 108 (2011) 249–264.
[29] H. Yamamoto, S. Tsuruoka, T. Ioka, H. Ando, C. Ito, T. Akimoto, et al., Indoxyl sulfate stimulates proliferation of rat vascular smooth muscle cells, Kidney Int. 69 (2006) 1780–1785.
[30] H. Shimizu, Y. Hirose, F. Nishijima, Y. Tsubakihara, H. Miyazaki, ROS and PDGF-beta [corrected] receptors are critically involved in indoxyl sulfate actions that promote vascular smooth muscle cell proliferation and migration, Am. J. Physiol. Cell Physiol. 297 (2009) C389–C396.
[31] A. Mozar, L. Louvet, P. Morliere, C. Godin, C. Boudot, S. Kamel, et al., Uremic toxin indoxyl sulfate inhibits human vascular smooth muscle cell proliferation, Ther. Apher. Dial. 15 (2011) 135–139.
[32] G. Muteliefu, H. Shimizu, A. Enomoto, F. Nishijima, M. Takahashi, T. Niwa, Indoxyl sulfate promotes vascular smooth muscle cell senescence with upregulation of p53, p21, and prelamin A through oxidative stress, Am. J. Physiol. Cell Physiol. 303 (2012) C126–C134.
[33] L.E. Dorn, L. Lasman, J. Chen, X. Xu, T.J. Hund, M. Medvedovic, et al., The m6A mRNA methylase METTL3 controls cardiac homeostasis and hypertrophy, Circulation 139 (2019) 533–545.
[34] J. Li, M.D. Kritzer, J.J. Michel, A. Le, H. Thakur, M. Gayanilo, et al., Anchored p90 ribosomal S6 kinase 3 is required for cardiac myocyte hypertrophy, Circ. Res. 112 (2013) 128–139.